Density Functional Investigation of Various States of the Molecules TcC, TcC_2, ScC_2, and YC_2

P. Jackson,* G. E. Gadd,† D. W. Mackey,‡ H. van der Wall,‡ and G. D. Willett*

School of Chemistry, The University of New South Wales, Sydney, NSW 2052, Australia

Received: November 24, 1997; In Final Form: April 20, 1998

Spin-polarized density functional theory has been used to investigate the C_{2v}, $C_{\infty v}$ and $D_{\infty h}$ isomers of the molecules MC_2, M = Sc, Y, Tc, and selected states of the diatomic molecule TcC. According to the theory, the ground state of the diatomic is the $^4\Sigma^+$ TcC isomer. Bond length comparisons between the doublet and quartet isomers reveal the ground state has a double bond, and the first excited state ($^2\Delta$ TcC) is triple bonded. For MC_2, M = Sc, Y, Tc, numerous minima were located, including spin states of the same symmetry. Cyclic isomers were identified as the ground states for each of the three metals. The minimized C−C bond length for $\tilde{X}\ ^2A_1$ TcC_2 is 1.58 Å, and is close to typical values for carbon−carbon single bonds, whereas the corresponding bond distances in $\tilde{X}\ ^2A_1$ MC_2, M = Sc, Y, are closer to typical values for carbon−carbon double bonds. Examination of the isomer structures and energies for TcC_2 suggests a preference for double bond formation with the carbon atoms of the C_2 unit. This is in contrast to scandium and yttrium dicarbides which prefer to form single bonds with the C_2 unit.

Introduction

The carbides of groups VIB−VIII elements exhibit polymorphism, and in many instances several phases have been isolated, for example, Cr_7C_3, Cr_3C_2, $Mn_{23}C_6$, $Mn_{15}C_4$, Mn_3C, Mn_5C_2, Mn_7C_3, Fe_3C, Fe_2C, MoC, and Mo_2C.[1] For technetium, the impure carbide phase TcC has been shown to be superconducting at 3.85 K.[2] To date, there have been no reports of the solid state synthesis of Tc_xC_y phases $x,y > 1$ and $x \neq y$; however, the 12-coordinate radius of Tc (136 pm)[3] suggests such phases might exist.[1] Furthermore, $TcC_{x\geq 2}$ molecules may be important precursors for the growth of such phases. On a molecular scale, the diatomic TcC has been detected in the vapor above a technetium−graphite melt.[4]

Our interest in the simple carbide molecules TcC and TcC_2 stems from spectroscopic investigations[5,6] of the ^{99m}Tc-labeled microaerosols Technegas[7] and Pertechnegas[8] used in the diagnosis of pulmonary disorders. The "99 m" is reference to the metastable isotope of technetium ($\tau_{1/2}$ = 6.02 h, γ = 140 keV, internal conversion)[9] that is widely used in single-photon emission computed tomography.[10] The metastable isotope decays to form a β-emitting isotope, ^{99}Tc, with $\tau_{1/2} = 2.13 \times 10^5$ years.[9]

Both the Technegas and Pertechnegas aerosols are generated by the graphite-assisted reduction (at 2800 K) of $Na^{99m}TcO_4$ in $Ar_{(g)}$ and 97% $Ar_{(g)}$/3% $O_{2(g)}$, respectively. Introduction of 3% O_2 into the $Ar_{(g)}$ stream results in an imaging agent with markedly different properties, notably a significantly shorter lung retention time. In a recent article,[5] Fourier transform ion cyclotron resonance mass spectrometry (FTICR−MS) and X-ray photoelectron spectroscopy (XPS) were used to identify some of the prevalent technetium-containing components of Pertechnegas which result from the reaction of water vapor with $Tc_2O_{7(g)}$, the gas phase analogue of the Tc(VII) starting material. In spite of several recent publications,[6,11,12] there is still controversy regarding the chemical form of the active component in the anoxic aerosol Technegas. FTICR−MS identification of fullerenes in the carbon soot collected at the patient outlet orifice of the aerosol generator led to early speculation that endohedral Tc−metallofullerenes may be responsible for the agent's properties in lung ventilation studies.[13]

The density functional studies detailed in this article were undertaken to ascertain the nature of technetium−carbon bonding in small molecules which may be directly linked to the growth of extended carbide phases or, perhaps, even precursors to the formation of metcar-type molecules.[14−17] For comparison with TcC_2, potential energy surface (PES) investigations have also been performed for ScC_2 and YC_2, two metals for which endohedral metallofullerenes have been detected. This could provide insight into the reasons why midtransition row metal atoms do not form metallofullerenes in the presence of gaseous carbon. In addition, we propose that C_2 units may be implicated in fullerene/metallofullerene assembly processes, and the evidence we cite includes the mass separation (24 *m*/*z* units, C_2 units) of $C_x^{+,-}$ peaks in cluster distributions generated using laser vaporization, and collision induced dissociation (CID) of carbon-cage molecules for which the loss of C_2 units, or multiples thereof, are observed.[18]

Theoretical Methods

Several texts and publications describe the application of density functional theory to molecular problems[19−23] with specific reference to the DMol approach in articles by Delley and Ellis[24] and by Delley.[25]

Geometry optimizations in this study were performed using local and nonlocal spin density functional theories as implemented in DMol 096 with a BLYP functional combination.[26] All minima were located using a quasi-Newton−Raphson energy searching procedure. Low energy structures and excited states were investigated for imaginary vibrational frequencies using central (4-point) differencing. For those structures exhibiting imaginary frequencies, geometry optimizations were performed until the rms gradient was less than 10^{-4}.

† Physics, Australian Nuclear Science and Technology Organization (ANSTO), Private Mailbag 1, Menai, NSW 2234, Australia.

‡ Department of Nuclear Medicine, Concord Repatriation Hospital, Concord, NSW 2139, Australia.

10.1021/jp980315p CCC: $15.00
Published on Web 10/10/1998

TABLE 1: Molecular Properties Calculated for Some Spin Isomers of TcC Using DFT and a Nonlocal BLYP Spin Density Functional Combination

state	T_e (cm^{-1})	r_e (Å)	ω_e (cm^{-1})	D_0(Tc−C) (eV)[a]	metal charge[b]
$^4\Sigma^+$	0	1.710	937	6.94	+0.47
$^2\Delta$	2742	1.663	1083	6.60	+0.35
$^2\Pi$	3541	1.733	887	6.51	+0.34
$^6\Pi$	23691	1.909	715	4.01	+0.50
octet			repulsive		

[a] Experimental value is 6.02 eV. From ref 4. [b] Charge calculated from the Mulliken population analysis in units of $q \times e$, where e is the fundamental unit of charge (1.602×10^{-19} C).

The BLYP functional combination[27,28] was used self-consistently in all ^{98}TcC, ScC_2, YC_2, and $^{98}TcC_2$ calculations, while the local correlation functional VWN,[29] in conjunction with the von Barth and Hedin modification of the Slater exchange functional,[30] was also used to investigate YC_2. The most extensive numerical basis sets available, that is, double numerical basis sets including 3p diffuse and 3d polarization functions for carbon, and 4sp, 5sp diffuse and polarization functions for the d^1, d^5 metals, respectively, were used in all of the calculations. The $n = 1$ shell of C, $n = 1,2$ shells of Sc, and the $n = 1-3$ shells of ^{98}Tc, Y (inactive cores) were frozen at the corresponding atomic charge densities, thus leaving an extensive, flexible valence region that should be sufficient to account for inner orbital relaxation upon bond formation. The extra fine mesh option was used for the evaluation of the exchange−correlation potential grid points, as well as the Coulomb contribution to the electron−electron interaction potential. The latter was evaluated using the Poisson method.

All bond energies and reaction enthalpies presented were derived from zero-point vibrational energy-corrected molecular binding energies. The major error sources should be the neglect of relativistic effects, which should not affect qualitative interpretations, and the approximation of the nondynamic or exchange electron correlation. The DFT geometries of ScC_2 and TcC_2 will provide good starting structures for future higher level, relativistic first-order configuration interaction calculations.

The DMol 096 calculations were performed on a Fujitsu VP-2200 housed at Australian Nuclear Science and Technology Organization, Sydney, and on a Silicon Graphics INDIGO workstation.

Results and Discussion

A. ^{98}TcC. Diatomic ^{98}TcC is the only carbide molecule of technetium for which a molecular property has been experimentally measured.[4] For this reason, we have chosen to investigate some of the diatomic spin states, in order to assess the performance of the density functional implementation. Diatomic binding energies can also be used to evaluate $^{98}TcC_2$ carbon atom extraction enthalpies. The density functional results for ^{98}TcC are presented in Table 1.

In the following discussion, it is assumed that the lowest energy state corresponding to each multiplicity has been located by the energy searching procedure.

The electronic configuration of the ground state ($^4\Sigma^+$ ^{98}TcC) is $...a\sigma^2a\pi^4b\sigma^2a\delta^2c\sigma^1$. The a$\sigma$ orbital has predominantly C 2s character and is essentially nonbonding, while the bσ orbital is ^{98}Tc $5p_z4d_{z^2}$/C $2p_z$ bonding with a small 5s contribution. The aπ orbitals are the ^{98}Tc $4d_{xz}$/C $2p_x$, ^{98}Tc $4d_{yz}$/C $2p_y$ π-bonding orbitals. The δ orbitals with occupation numbers of 1.00 correspond to the nonbonding $4d_{x^2-y^2}$, $4d_{xy}$ electrons, while the SOMO (cσ) has predominantly ^{98}Tc 5s/C $2p_z$ character.

The dominant ground state metal−carbon bonding contributions are the $(4d-2p)\pi$ and $(2p_z-4d_{z^2})\sigma$. The strongest C 2s interactions are with the 4s, $5p_z$ orbitals of ^{98}Tc, according to the Mulliken overlap populations (0.029 (↑), 0.033 (↓) for 4s and 0.043 (↑), 0.012 (↓) for $5p_z$, respectively), which is evidence that dπ−pπ bonding must be important for molecular stabilization, as the σ-type values are small relative to the $2p_x-4d_{xz}$ and $2p_y-4d_{yz}$ π values (0.078 (↑), 0.096 (↓)). Interestingly, the $2s-4d_{z^2}$ and $2s-4p_z$ overlap populations are comparable (0.018 (↑), 0.018 (↓) and 0.017 (↑), 0.016 (↓), respectively).

The MO overlap populations also reveal that the 4p electrons of ^{98}Tc should not be considered "core" electrons (0.018 (↑), 0.018 (↓) for $2s-4p_z$, and 0.012 (↑), 0.016 (↓) for $2p_z-4p_z$), and should be included as part of the valence or active electron region in any theoretical calculations for Tc-containing molecules. The bonding involvement of the 5p diffuse functions of ^{98}Tc also suggests higher angular momentum functions may need to be incorporated in the metal basis set for high precision energetics.

An unusual result is the shorter bond length and higher vibrational frequency of the first excited state (2Δ ^{98}TcC, see Table 1), with respect to the ground state. It is more often observed that ground state isomers have shorter bond length(s) and higher vibrational frequency/frequencies.

The dissociation energy of the ground state, after zero-point vibrational energy correction, is 6.94 eV. The dissociation energy of TcC has been determined experimentally, using electron ionization−Knudsen effusion mass spectrometry, to be 6.02 ± 0.1 eV.[4] Numerous approximations were used in the evaluation of the experimental dissociation energy, including the estimation of $(H^\circ_{2450} - H^\circ_0) = 0.89$ eV, the Gibbs free energy functions for $C_{(s)}$,$Tc_{(g)}$ and the estimation of appearance energies for Tc^+ and TcC^+ (±0.2 eV, ±0.5 eV, respectively). Furthermore, the "equilibrium" assumption does not take into account fragmentations of higher carbides that lead to the formation of TcC. It should be noted that C_2 and C_3 are the most prevalent molecular species in carbon vapors over the experimental temperature range[31] and that an extension of the present investigation has established that TcC_3 is also a stable molecule.[32] Even though the DFT dissociation energy value appears to be too high by approximately 0.8 eV, the cited uncertainty in the experimental value appears to be too small. On the basis of $\Delta E = D_0(MoC)_{expt} - D_0(MoC)_{BLYP}$, for $\tilde{X}$ $^3\Sigma^-$ MoC, the "calibrated" nonlocal-DFT value for TcC is 6.84 eV. Molecular beam dissociation studies are required to resolve the accuracy of the non-state-selective effusion measurement and the DFT values.

It can be argued that nonrelativistic DFT might be unreliable for the calculation of binding energies for second-row transition metal-containing molecules. In order to test this idea and to calibrate the theoretical results for TcC, we also used the same level of theory (NLSD/BLYP) for the calculation of the ground state of $^3\Sigma^-$ MoC ($Z = 42$, Mo; cf. $Z = 43$, Tc). The experimental bond dissociation energy of MoC, 5.30 ± 0.11 eV, can be determined using the relationship $D_0(MoC) = IE(MoC) - IE(Mo) + D_0(Mo^+-C)$, and the values, IE(Mo) = 7.09243 eV, [33] IE(MoC) = 7.73 ± 0.26 eV,[34] and $D_0(Mo^+-C) = 4.66 \pm 0.11$ eV.[34] The theoretical dissociation energy value of 5.4 eV ($^3\Sigma^-$ MoC,...$1\sigma^21\pi^42\sigma^21\delta^23\sigma^0$), $r_e = 1.738$ Å, $\omega_e = 857$ cm^{-1}, binding energy = 126.8 kcal mol^{-1}), is within the uncertainty of the experimental result.

Using the results from Table 1, the energy required to produce a single bond from the double bond in $\tilde{X}$ $^4\Sigma^+$ ^{98}TcC is 2.94 eV,

TABLE 2: Molecular Properties Calculated for Isomers of TcC_2 Using DFT and a Nonlocal BLYP Spin Density Functional Combination

state	T_e (cm^{-1})	r_e (M−C) (Å)	r_e (C−C) (Å)	∠C−M−C°	M^{+q} q^a	C^{-q} q^a
$^2A_1$	0	1.791	1.581	52.4	0.66	0.33
$^6A_1$	4751	1.995	1.291	36.6	0.64	0.32
$^4B_1$	6069	1.995	1.392	40.8	0.66	0.33
$^8A_1$	21121	2.374	1.269	31.0	0.44	0.22
$^6\Delta$	3225	1.880	1.313	180.0	0.63	0.44, 0.19[b]
$^4\Pi$	9468	1.854	1.357	180.0	0.54	0.34, 0.20[b]
$^2\Sigma^+$	13179	1.831	1.347	180.0	0.47	0.24, 0.23[b]
$^8\Sigma^+$	24867	2.083	1.245	180.0	$\omega_{im} = 175i$ cm^{-1} (π)	
$^6\Sigma_g^+$	32497	1.847		180.0	0.62	0.31
$^2\Sigma_g^+$	33547	1.894		180.0	$\omega_{im} = 365i$ cm^{-1} (π_u)	
$^4\Delta_g$	35471	1.923		180.0	$\omega_{im} = 447i$ cm^{-1} (σ_u^+)	
$^8\Pi_g$	45849	1.914		180.0	0.64	0.32

[a] Atomic charges are given in units of $q \times e$, where e is the fundamental unit of charge (1.602×10^{-19} C). [b] The first charge is for the central carbon atom (bonded directly to the metal), while the second charge is for the terminal carbon atom.

and the energy required to produce a triple bond from the double bond is 0.34 eV.

B. $^{98}TcC_2$. Comparison of the experimental dissociation energy, $D_0(^{99}TcC) = 6.02 \pm 0.1$ eV, and the analogous value for the dicarbon molecule, $D_0(C_2) = 6.06 \pm 0.04$ eV,[35] suggests there will be some degree of C−C bonding in low energy metal−dicarbide isomers. Furthermore, if MC_2 molecules act as templates for the growth of fullerene cages, the $^{98}Tc-C_2$ interactions should maintain the multiple-bond character of the C_2 molecule to some extent, and so the $D_{\infty h}$ insertion isomers should be relatively unstable with respect to the C_{2v}, $C_{\infty h}$ isomers. It has recently been proposed that certain midrow transition metals may inhibit cage formation by attacking 5-membered carbon rings, thus catalyzing the growth of nanotube formations.[36−38]

Three principle geometric structures for $^{98}TcC_2$ were investigated: metal insertion structures, CTcC, with $D_{\infty h}$ symmetry, cyclic structures with C_{2v} symmetry, and metal−acetylide structures with $C_{\infty v}$ symmetry. C−C bonding is seen to be a feature of both C_{2v} and $C_{\infty v}$ structures, but is absent in $D_{\infty h}$ structures.

The results of the calculations reveal that spin isomers of all three geometries are minima on the potential energy hypersurface (PES). The molecular properties, including the bond lengths, bond angles, Mulliken atomic charges, and relative energies with respect to the ground state, for each of the isomers and saddle point structures, are presented in Table 2.

The ground state $^{98}TcC_2$ structure is cyclic $^2A_1$, with the nearest excited state corresponding to the $^6\Delta$ linear (metal−acetylide) structure. The relative isomer energies and carbon−carbon bond lengths reveal that weakening of the C_2 bond is energetically favored, as is formation of $^{98}Tc-C$ double bonds in both the cyclic and linear structures. The molecular orbitals contributing to the metal−carbon double bond character in the ground state isomer are $^{98}Tc\ 4d_{z^2}/C\ 2p_x$ (σ-type), $^{98}Tc\ 4d_{x^2-y^2}/C\ 2p_z$ (σ-type), and $^{98}Tc\ 4d_{xy}/C\ 2p_y$ (π-type).

Unlike the cyclic structures for which the low spin isomer was most stable, the high spin sextet $C_{\infty v}$ structure was the lowest energy linear isomer. The instability of terminal divalent carbon atoms is suggested by the relative instability of the linear insertion isomers, the most stable of which is the sextet (see Table 2). The electron configurations, harmonic vibrational frequencies and molecular atomization energies of the various isomers are presented in Table 3.

TABLE 3: Molecular Properties Calculated for Isomers of TcC_2 Using DFT and a Nonlocal BLYP Spin Density Functional Combination.[a]

C_{2v}	electron configuration	ω_e (cm^{-1}) b_1	a_1	a_1	$\Delta H_{0,at}$ ($TcC_2 \rightarrow$ Tc + 2C) (eV)
$^2A_1$	$...a_1^2a_1^2b_1^2b_1^2a_2^2a_1^1$	389	729	1010	12.48
$^4B_1$	$...a_1^2a_2^1b_1^2b_1^2a_1^1b_2^1$	499	446	1258	11.72
$^6A_1$	$...a_2^1a_1^1b_1^1b_2^1a_1^1$	565	361	1672	11.86
$^8A_1$	$...b_2^2a_1^1a_2^1b_1^1a_1^1b_2^1a_1^1a_1^1$	337	171	1819	9.85

$C_{\infty v}$	electron configuration	ω_e (cm^{-1}) π	σ	σ	$\Delta H_{0,at}$ ($TcC_2 \rightarrow$ Tc + 2C) (eV)
$^2\Sigma^+$	$...\sigma^1$	154	532	1346	10.84
$^4\Pi$	$...\delta^2\pi^3\sigma^0$	279	526	1504	11.27
$^6\Delta$	$...\pi^4\delta^3\sigma^1\sigma^1\pi^2$	293	547	1684	12.05

$D_{\infty h}$	electron configuration	ω_e (cm^{-1}) π_u	σ_u^+	σ_u^+	$\Delta H_{0,at}$ ($TcC_2 \rightarrow$ Tc + 2C) (eV)
$^6\Sigma_g^+$	$...\sigma_g^2\delta_g^2\pi_u^2\sigma_g^1$	187	497	749	8.68
$^8\Pi_g$	$...\delta_g^1\pi_u^1\delta_g^1\ \pi_u^2\sigma_u^1\ \sigma_g^1$	151	518	764	7.12

[a] The π vibrational mode of the $C_{\infty v}$, $D_{\infty h}$ isomers is degenerate. [b] From ref 35.

TABLE 4: Molecular Properties Calculated for Isomers of ScC_2 and YC_2 Using DFT and Local SVWN and Nonlocal BLYP Spin Density Functional Combinations[a]

method[b]	state	T_e (cm^{-1})	r_e (M−C) (Å) **(ScC_2)**	r_e (C−C) (Å)	∠C−M−C°
	$^2A_1$	0	2.063	1.279	36.1
	$^4A_2$	16162	2.215	1.286	33.8
	$^2\Sigma^+$ [c]	5237	1.945	1.291	180.0
	$^2\Pi_u$ [d]	47861	1.897		180.0
	$^4\Sigma_g^+$	48069	1.970		180.0

method[b]	state	T_e (cm^{-1})	r_e (M−C) (Å) **(YC_2)**	r_e (C−C) (Å)	∠C−M−C°
NLSD	$^2A_1$	0	2.215	1.276	33.5
LSD		0	2.180	1.272	33.9
FOCI		0	2.223	1.277	33.2
NLSD	$^4B_1$	17719	2.318	1.297	32.5
LSD		18555	2.293	1.305	33.1
FOCI		22022	2.637	1.313	28.8
NLSD	$^2\Sigma^+$	4606	2.076	1.290	180.0
LSD		8358	2.092	1.295	180.0
FOCI		4300	2.087	1.281	180.0
NLSD	$^2\Pi_u$ [e]	50540	1.989		180.0
LSD		50739	1.965		180.0
NLSD	$^4\Pi_g$	50553	1.988		180.0
LSD[f]		53410	1.985		180.0

[a] The FOCI results for YC_2 are from ref 39. [b] All results for ScC_2 from NLSD/BLYP calculations. [c] Corresponds to a saddle point on the PES, $\omega_{im} = 159i$ cm^{-1}, π bending mode. [d] Corresponds to a saddle point on the PES, $\omega_{im} = 211i$ cm^{-1}, $613i$ cm^{-1}. [e] Corresponds to a saddle point on the PES, $\omega_{im} = 200i$ cm^{-1} (NLSD), $104i$ cm^{-1} (LSD), π_u bending mode. [f] Corresponds to a saddle point on the LSD PES, $\omega_{im} = 55i$ cm^{-1}, π_u bending mode.

An upper bound to the enthalpy of the reaction

$$\Delta H_{0,r}: \ ^{98}TcC_2 \rightarrow {}^{98}TcC + C$$

is calculated to be 5.55 eV.

C. Potential Energy Surface Maps for MC_2, M = Sc, Y. Molecular properties for the various minima and transition structures of C_{2v}, $C_{\infty v}$, and $D_{\infty h}$ symmetry for ScC_2 and YC_2 are given in Table 4.

Investigations of the quartet $C_{\infty v}$ structures of both Sc, Y were plagued by oscillatory SCF energy behavior over a range of

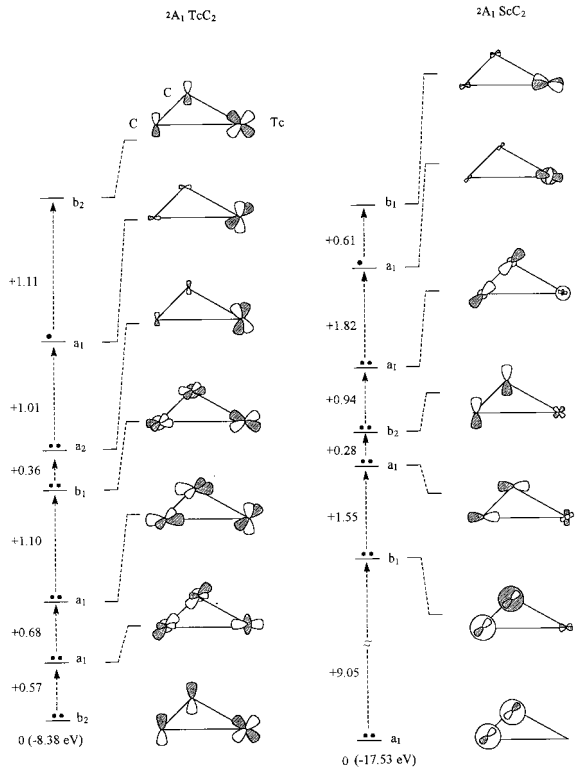

Figure 1. Qualitative pictorial representation of some of the valence molecular orbitals of the ground state isomers of TcC_2 and ScC_2. Atomic orbital contributions to individual molecular orbitals are to scale. Energy separations between occupied levels are given in eV and are referenced to the eigenvalue of the lowest energy molecular orbital shown for each molecule. The covalent nature of the interaction of C 2p/ Tc 4d orbitals leads to a significant reduction of the dicarbon bond order in TcC_2.

bond lengths, and as an earlier first-order configuration interaction (FOCI-HF) study of some YC_2 structures[39] has revealed, the most stable multiplicity for these molecules is two. The PES search for these isomers was therefore discontinued. LSD investigations of the molecular topology confirm the FOCI-HF result of enhanced stability for cyclic, or bridging structures, for YC_2. The doublet spin state and cyclic structures are also favored by Sc. With the exception of $^4\Sigma_g^+$ ScC_2, all of the insertion structures for Sc, Y were found to be saddle points (see Table 4). Furthermore, $^4\Sigma_g^+$ ScC_2 was the only linear minimum located for Sc. The preservation of the C−C double bond character in the ground state structures for ScC_2, YC_2 was also noted, in contrast to the reduced C−C bond order (single bond) in ground state $^{98}TcC_2$. The local density functional energy difference between the $^2A_1$ and $^2\Sigma^+$ isomers of YC_2 is 1.04 eV, which is in fair agreement with the first order configuration interaction (FOCI) result of 0.682 eV,[39] considering 53 000 configuration spin functions, along with a relativistic effective core potential, were used in the FOCI calculation. The nonlocal result (0.57 eV) is in better agreement with the FOCI value. The quality of the results obtained for the ScC_2 isomers (lighter d^1 metal) should be comparable to the nonlocal results for YC_2; however, more experimental measurements are required before a critical assessment of nonlocal DFT for the excitation energies of $^{98}TcC_2$ isomers is possible.

Figure 1 is a qualitative pictorial representation of the atomic orbital contributions to the molecular orbitals for the ground states of ScC_2 and $^{98}TcC_2$. The character of the MO's of ground state YC_2 and ScC_2 isomers are similar, but have slightly different energy separations, and for this reason the results for YC_2 are not presented. There is much greater C 2p/M 4d atomic orbital interaction within the MO's of $^{98}TcC_2$ than ScC_2, for which there is either little M−C orbital mixing or significant back-bonding, leading to the formation of polar bonds.

TABLE 5: Comparison of the Theoretical (NLSD, LSD, and FOCI) and Experimental Atomization Energies and Metal−Dicarbon Bond Dissociation Energies for the ScC_2, YC_2 Isomers

	$\Delta H_{0,at}$: $MC_2 \rightarrow M + 2\ C$ (eV)			$\Delta H_{0,r}$: $MC_2 \rightarrow M + C2$ (eV)		
		lit.			lit.	
state	DFT	theoretical	exptl	DFT[a]	theoretical	exptl
			ScC_2[b]			
$^2A_1$	12.70		12.3[c]	6.64		6.1[c]
$^4A_2$	10.72					
$^4\Sigma_g^+$	6.73					
			YC_2			
$^2A_1$	12.94 (NLSD)	11.675[d]	12.9[e,f]	6.88 (NLSD)	6.948[d]	6.7[h]
	14.87 (LSD)		12.7[g]	8.81 (LSD)		
$^4B_1$	10.76 (NLSD)			4.70 (NLSD)		
	12.59 (LSD)			6.53 (LSD)		
$^2\Sigma^+$	12.37 (NLSD)	10.993[d]		6.31 (NLSD)	6.266[d]	
	13.86 (LSD)			7.80 (LSD)		
$^4\Pi_g$	6.76 (NLSD)			0.70 (NLSD)		

[a] Calculated using the experimentally determined $D_0(C_2) = 6.06$ eV, from ref 35. [b] All ScC_2 DFT results from the NLSD/BLYP calculations of this work. [c] Experimental result from ref 42. [d] FOCI result from ref 39. [e] Experimental result from ref 43. [f] Experimental result from ref 44. [g] Experimental result from ref 45. [h] Experimental result from ref 46.

The theoretical enthalpies of atomization ($\Delta H_{0,atom}$) and the metal−dicarbon bond dissociation energies $D_0(M-C_2)$ for M = Sc, Y are presented in Table 5. Although the theoretical $M-C_2$ bond strengths for the ground states of $^{98}TcC_2$ and ScC_2 are close, the value for $^{98}TcC_2$ is expected to be overestimated by ~0.7 eV if the difference between the theoretical and experimental values for the dissociation energy of TcC are a true reflection of the accuracy of nonlocal-DFT. Hence the metal−dicarbon interaction in ScC_2 is considerably stronger than for the d^5 metal. As expected, both the metal−dicarbon bond-dissociation energy and the atomization energy calculated for YC_2 using the local spin density approximation (LSD/SVWN) are overestimated and compare poorly with both FOCI and experimental results. The magnitude of the LSD overbinding error should vary little from the cyclic to linear isomers for a particular metal; hence, the predicted excitation energy $^2\Sigma^+ \leftarrow {}^2A_1$ compares reasonably well with the FOCI result.

On the basis of the computational results presented in this paper, it appears that Tc prefers to bridge dicarbon and reduce the C−C bond order to 1 through the formation of metal−carbon double bonds (olefin activation). In contrast, Sc, Y interact with dicarbon via polar (single) bonds and maintain C−C π bonding to some extent. The covalent nature of the metal−dicarbon interaction in $^2A_1$ TcC_2 is supported by the charge density redistribution plot (see Figure 2). The charge density redistribution plot depicts a spatial dependence of the charge density, or more precisely, the difference between the density distribution in the molecule, and the density distribution of the unperturbed atoms in the molecular configuration. For $^2A_1$ TcC_2, there is clearly a build up of charge density along the Tc−C bonds, and also along the C−C bond. In contrast, $^2A_1$ YC_2 exhibits no build up along the Y−C bonds, but there is significant charge concentration along the C−C bond, and the diffuse nature of this density probably reflects the greater degree of π bonding in the C_2 unit. We conclude that the $Y-C_2$ interaction is predominantly electrostatic.

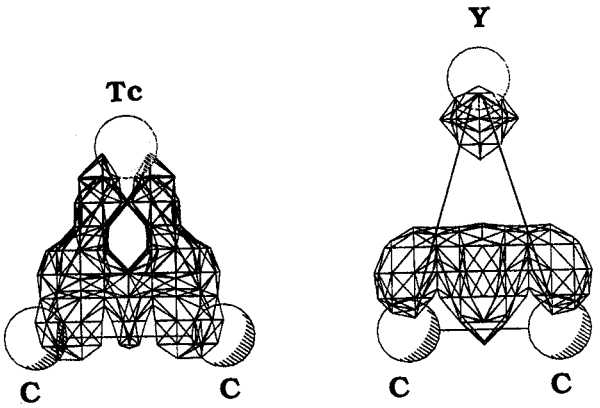

Figure 2. Charge density deformation contours for $^2A_1$ TcC_2 and $^2A_1$ YC_2 obtained from nonlocal DFT calculations employing the BLYP functional combination.

There appears to be a propensity for d^1 metals to energetically favor structures that bridge, and maintain the conjugated integrity, of carbon−carbon bonds. This has been confirmed by other theoretical investigations.[39−41] Under the conditions favored for endohedral fullerene formation, incorporation of cyclic MC_2 units, M = Sc, Y, into carbon cage during cluster growth may ultimately lead to encapsulation.

Olefinic C−C bond activation by the midtransition row metal suggests the formation of endohedral technetium fullerenes is unlikely. Other high-valence metals may attack conjugated carbon systems in a similar fashion.

Acknowledgment. P.J. is grateful to the Nuclear Medicine Research Foundation (c/-Dr. Hans van der Wall, Department of Nuclear Medicine, Concord Repatriation Hospital, Concord, NSW, Australia) and the Australian Institute of Nuclear Science and Engineering for financial support. We also acknowledge support from the Australian Research Council. A generous computer time allocation from the Australian Nuclear Science and Technology Organization is gratefully acknowledged. We are also indebted to Prof. Ian Dance (UNSW) for access to the SG workstation and software, and Dr. Keith Fisher (UNSW) for helpful comments.

References and Notes

(1) Greenwood, N. N.; Earnshaw, A. *Chemistry of the Elements*; Pergamon Press: New York, 1993; p 320.
(2) Giorgi, A. L.; Szklarz, E. G. *J. Less-Common Met.* **1966**, *11*, 455.
(3) Knittel, C. *Introduction to Solid State Physics*, 6th ed.; John Wiley & Sons: New York, 1986; p 76.
(4) Rinehart, G. H.; Behrens, R. G. *J. Phys. Chem.* **1979**, *83*, 2052.
(5) Mackey, D. W. J.; Jackson, P.; Baker, R. J.; Dasaklis, C.; Fisher, K. J.; Magee, M.; Bush, V.; Burch, W. M.; van der Wall, H.; Willett, G. D. *J. Nucl. Med.* **1997**, *38*, 163.
(6) Jackson, P.; Baker, R. J.; McCulloch, D. G.; Mackey, D. W. J.; van der Wall, H.; Willett, G. D. *Nucl. Med. Commun.* **1996**, *17*, 504.
(7) Burch, W. M.; Sullivan, P. J.; McLaren, C. J. *Nucl. Med. Commun.* **1986**, *7*, 865.
(8) Monaghan, P.; Murray, I. P. C.; Mackey, D. W. J.; van der Wall, H.; Walker, B. M.; Jones, P. D. *J. Nucl. Med.* **1991**, *32*, 1945.
(9) Heath, R. L. *Handbook of Chemistry and Physics*; Weast, R. C., Ed.; CRC Press: Boca Raton, 1986.
(10) Ott, R. J.; Flower, M. A.; Babich, J. W.; Marsden, P. K. *The Physics of Medical Imaging*; Webb, S., Ed.; Medical Science Series, Institute of Physics Publishing: Bristol, 1995; p 142.
(11) Isawa, T.; Lee, B. T.; Hiraga, K. *Nucl. Med. Commun.* **1996**, *17*, 147.
(12) Lloyd, J. J.; Shields, R. A.; Taylor, C. J.; Lawson, R. S.; James, J. M.; Testra, H. J. *Eur. J. Nucl. Med.* **1995**, *22*, 473.
(13) Mackey, D. W. J.; Burch, W. M.; Dance, I. G.; Fisher, K. J.; Willett, G. D. *Nucl. Med. Commun.* **1994**, *15*, 430.
(14) Guo, B. C.; Kerns, K. P.; Castleman, A. W., Jr. *Science* **1992**, *233*, 1411.
(15) Wei, S.; Guo, B. C.; Purnell, J.; Buzza, S. A.; Castleman, A. W., Jr. *Science* **1992**, *256*, 818.
(16) Wei, S.; Guo, B. C.; Purnell, J.; Buzza, S. A.; Castleman, A. W., Jr. *Science* **1992**, *256*, 515.
(17) Wei, S.; Guo, B. C.; Buzza, J.; Castleman, A. W., Jr. *J. Phys. Chem.* **1992**, *96*, 4166.
(18) Weiss, F. D.; O'Brien, S. C.; Elkind, J. L.; Curl, R. F.; Smalley, R. E. *J. Am. Chem. Soc.* **1988**, *110*, 4464.
(19) Parr, R. G.; Yang, W. *Density Functional Theory of Atoms and Molecules*; Oxford University Press: Oxford, 1995.
(20) Seminario, J. M.; Politzer, P., Eds. *Modern Density Functional Theory: A Tool for Chemistry*; North-Holland: Amsterdam, 1995.
(21) Ellis, D. E., Ed. *Density Functional Theory of Molecules, Clusters and Solids*; Kluwer Academic: Amsterdam, 1994; Vol. 12.
(22) Zeigler, T. *Chem. Rev.* **1991**, *91*, 651.
(23) Jones, R. O.; Gunnarsson, O. *Rev. Mod. Phys.* **1989**, *61*, 689.
(24) Delley, B.; Ellis, D. E. *J. Chem. Phys.* **1982**, *76*, 1949.
(25) Delley, B. *Modern Density Functional Theory: A Tool for Chemistry*; Seminario, J. M., Politzer, P., Eds.; North-Holland: Amsterdam, 1995; p 221.
(26) DMol, version 4; MSI Software: San Diego, 1996.
(27) Lee, C.; Yang, W.; Parr, R. G. *Phys. Rev. B.* **1988**, *37*, 785.
(28) Becke, A. D. *Phys. Rev. A.* **1988**, *38*, 3098.
(29) Vosko, S. J.; Wilk, L.; Nusair, M. *Can. J. Phys.* **1980**, *58*, 1200.
(30) Slater, J. C. *Int. J. Quantum Chem., Quantum Chem. Symp.* **1975**, *9*, 7.
(31) Leider, H. R.; Krikorian, O. H.; Young, D. A. *Carbon* **1973**, *11*, 555.
(32) Jackson, P.; Mackey, D. W.; van der Waal, H.; Willett, G. D.1998. Unpublished results.
(33) Rayner, D.; Mitchell, S. A.; Bourne, O. L.; Hackett, P. A. *J. Opt. Soc. Am.* **1987**, *B4*, 900.
(34) Sievers, M. R.; Chen, Y.-M.; Armentrout, P. B. *J. Chem. Phys.* **1996**, *105*, 6322.
(35) Huber, K. P.; Herzberg, G. *Molecular Spectra and Molecular Structure IV. Constants of Diatomic Molecules*; Van Nostrand Reinhold Co.: New York, 1979.
(36) Guo, T.; Nikolaev, P.; Thess, A.; Colbert, D. T.; Smalley, R. E. *Chem. Phys. Lett.* **1995**, 49.
(37) Thess, A.; Lee, R. N.; P.; Dai, H. J.; Petit, P.; Robert, J.; Xu, C. H.; Lee, Y. H.; Kim, S. G.; Rinzler, A. G.; Colbert, D. T.; Scuseria, G. E.; Tomanek, D.; Fischer, J. E.; Smalley, R. E. *Science* **1996**, *273*, 483.
(38) Dai, H. J.; Rinzler, A. G.; Nikolaev, P.; Thess, A.; T., C. D.; Smalley, R. E. *Chem. Phys. Lett.* **1996**, *260*, 471.
(39) Roszak, S.; Balasubramanian, K. *Chem. Phys. Lett.* **1995**, *246*, 20.
(40) Strout, D. L.; Hall, M. B. *J. Phys. Chem.* **1996**, *100*, 18007.
(41) Roszak, S.; Balasubramanian, K. *J. Chem. Phys.* **1997**, *106*, 158.
(42) Haque, R.; Gingerich, K. A. *J. Chem. Phys.* **1981**, *74*, 6407.
(43) Wagman, D. D.; Evans, W. H.; Parker, V. B.; Schumm, R. H. The NBS Tables of Chemical Thermodynamic Properties. NBS Technical Note 270. *J. Phys. Chem. Ref. Data* **1982**, Suppl. 1, 1.
(44) De Maria, G.; Guido, M.; Malspina, L.; Pesce, B. *J. Chem. Phys.* **1965**, *43*, 4449.
(45) Kohl, F. J.; Stevens, C. A. *J. Chem. Phys.* **1970**, *52*, 6310.
(46) Haque, R.; Gingerich, K. A. *J. Chem. Soc., Faraday Trans. II* **1979**, 982.